

NUMERICAL ASSESSMENT ON HEAT TRANSFER PERFORMANCE OF DOUBLE-LAYERED OBLIQUE FINS MICRO-CHANNEL HEAT SINK WITH Al_2O_3 NANOFLUID

by

Ji Ying CHOONG, Kok Hwa YU*, and Mohd Zulkifly ABDULLAH

School of Mechanical Engineering, Engineering Campus,
University Sains Malaysia, Penang, Malaysia

Original scientific paper
<https://doi.org/10.2298/TSCI200822142C>

This paper demonstrates a numerical study on heat transfer characteristics of laminar flow in a double-layered oblique finned heat sink using nanofluids with Al_2O_3 nanoparticles. Micro-channel heat sink with primary channel width of 0.5 mm with aspect ratio of 3 is employed. Instead of having conventional straight fins, oblique fins with narrow secondary channels are used. In this numerical study, single-phase fluid model with conjugate heat transfer is considered. The numerical modeling was first validated with existing data for double-layered conventional micro-channel heat sink having water (base fluid) as the working fluid. Numerical investigations on oblique finned micro-channel heat sink were then conducted for flow rates ranging from $3 \cdot 10^{-7}$ to $15 \cdot 10^{-7}$ m³/s, equivalent to primary channel inlet velocity in between 0.2 and 1.0 m/s. It was found that double-layered oblique finned configuration yields better heat transfer performance, inferred by the lower overall thermal resistance obtained as compared with that of double-layered conventional heat sink. Employing double-layered oblique finned heat sink, the heat transfer performance could be further enhanced, by using nanoparticles that are added into water-based fluid. It is found that the reduction of overall thermal resistance is proportional to the volume fraction of nanoparticles. Using cross-flow double-layered oblique finned configuration, the largest reduction in the overall thermal resistance can reach up to 25%, by using nanofluids with 4% volume fraction of Al_2O_3 nanoparticles.

Key words: laminar flow, conjugate heat transfer, CFD, nanoparticles, thermal resistance

Introduction

The evolution of electronics technology is leading IC chips toward smaller scale and dense circuit integration that often generates high heat intensity. Single-layered micro-channel heat sink (SL-MCHS) was first introduced by Tuckerman and Pease [1], which demonstrated the capability of a small, very compact, water cooled integrated heat sink for large heat dissipation. The disadvantage of SL-MCHS is the non-uniform temperature distribution along the heat sink, which induces unwanted thermal stresses in microelectronic systems. Besides, high temperature gradient observed in SL-MCHS limits the capability of heat dissipation in the microelectronic systems.

* Corresponding author, e-mail: yukokhwa@usm.my

Vafai and Zhu [2] proposed the concept of double-layered micro-channel heat sink (DL-MCHS) in which two SL-MCHS were stacked with one top of the other. This design was found to reduce the rise in temperature as the temperature attained is more uniformly distributed as compared with SL-MCHS design. In DL-MCHS, coolant can be forced in top channel in parallel direction with that of bottom channel (parallel flow) or in opposite direction (counter flow). Counter flow configuration for DL-MCHS was proposed by Wei *et al.* [3] who reported promising results in heat transfer. This design has resulted in better temperature uniformity as compared with parallel flow arrangement. Some existing studies reported that the heat transfer performance can be further enhanced by optimizing the geometric design parameters [4-7]. Apart from double-layered parallel flow and counter flow arrangement, Ansari and Kim [8] analyzed the heat transfer performance of a DL-MCHS with transverse flow configurations. Their study revealed that transverse flow configuration showed better temperature uniformity and lower overall thermal resistance as compared with parallel and counter flow in DL-MCHS. Toh *et al.* [9] performed a numerical study on micro-channel and reported that smaller friction factor can be expected at low Reynolds numbers, arising from lower water viscosity caused by high water temperature. Knight *et al.* [10] performed a study on the heat sink to investigate the effects of flow behavior in laminar and turbulent regime, revealing that laminar flow yielded a lower thermal resistance value over turbulent flow. Apart from having conventional fins, oblique finned SL-MCHS was proposed by Lee *et al.* [11, 12] and high heat transfer enhancement has been demonstrated, arising from chaotic fluid mixing induced by the sectional oblique fins.

Besides geometric parameters, thermal properties of coolant play important role in advanced thermal applications. Nanofluids with superior thermal properties such as TiO_2 , Al_2O_3 , and SiO_2 were extensively studied by researchers and often reported to enhance convective heat transfer performance significantly [13, 14]. Chein and Chuang [15] demonstrated that employing small volume fraction of CuO-water nanofluid would allow more heat energy to be absorbed and thus lower temperature is attained than that of coolant using pure water. A direct comparison of the thermophysical properties such as thermal conductivity and viscosity that are dominating the convective heat transfer of different nanofluids were documented by Iqbal *et al.* [16]. This study shows that the superior thermal conductivity of nanofluid could enhance the heat transfer of the system but adversely, it increases the pressure drop and pumping power due to increase in viscosity in nanofluids.

Numerical studies pertaining to laminar flow and convective heat transfer using nanofluids have been performed by researchers in different geometries, *i.e.*, triangular ducts [17], circular tube [18], and oblique finned micro-channel [19]. Ting and Hou [17, 18] reported that the utilization of nanofluids led to heat transfer enhancement in circular and triangular ducts under laminar flow regime. Furthermore, Tiwary *et al.* [19] studied the heat transfer characteristics of nanofluid in oblique finned SL-MCHS proposed by Lee *et al.* [11]. This recent study found that lower temperature variation was observed at the substrate of oblique finned channel as compared with rectangular channel which results in better heat transfer performance.

With thermal management issues often encountered in many industries, especially in electronic cooling, which demands extreme heat dissipation exceeding 1 kW/cm^2 . Thus, the objective of this study is focused on investigation of heat transfer characteristics for oblique finned DL-MCHS using water and Al_2O_3 nanofluid in different volume concentration. This could give some insights on the potential of oblique finned DL-MCHS for thermal management applications. In this study, a counter flow configuration of oblique finned DL-MCHS is numerically explored. The Al_2O_3 -water nanofluid is employed as the working fluid medium in the numer-

ical model. Coolant flows across the MCHS was assumed to be laminar where the maximum Reynolds number was kept less than transitional Reynolds number. Numerical simulation was performed for the entire conjugate heat transfer domain using ANSYS FLUENT 18.1.

Mathematical model

Geometrical configuration and boundary condition

Figure 1 shows arrays of oblique fins [11, 12] with main channel width of 500 μm were stacked up to form a DL-MCHS. The DL-MCHS dimensions were stated in tab. 1. The DL-MCHS is assumed to be made of copper with constant thermophysical properties, *i.e.*, density $\rho_s = 8.978 \cdot 10^3 \text{ kg/m}^3$, specific heat $c_s = 381 \text{ J/kgK}$ and thermal conductivity $k_s = 387.6 \text{ W/mK}$.

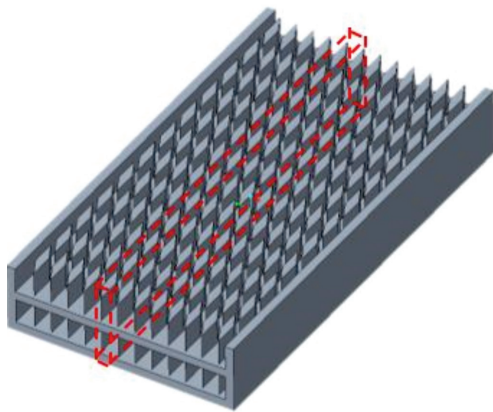


Figure 1. Schematic of oblique finned DL-MCHS

Table 1. Dimension details for DL-MCHS

Characteristic	Micro-channel dimension
Material	Copper
Footprint, width \times length [mm]	25 \times 25
Main channel width [μm]	500
Fin width [μm]	500
Channel depth [μm]	1500
Aspect ratio	3
Bottom thickness of substrate [μm]	500
Middle thickness of substrate [μm]	500
Number of fin per row	12
Fin pitch [μm]	2000
Fin length [μm]	1450
Oblique finned angle [$^\circ$]	27

Arising from the geometry periodicity of the oblique fins in the spanwise direction, the computational domain of the simulation model can be reduced to consider one periodic array of oblique fins arrangement, as indicated by the dashed lines in fig. 1. In this study, parallel flow (PF) and counter flow (CF) configuration of oblique finned DL-MCHS are investigated. The simplified model and boundary conditions employed on both cases are shown in fig. 2. On both sides (*i.e.*, left and right boundaries) of the simulation model, periodic boundary condition was adopted. It should be noted that the inlet of oblique finned DL-MCHS was extended to ensure the fluid-flow is fully developed before entering the MCHS, while its outlet was extended to prevent the occurrence of reverse flow when the fluid exiting the MCHS.

In this study, numerical investigations were conducted under the assumption of laminar flow regime with the total flow rates over top and bottom channels of a single periodic array of oblique fins arrangement, ranging from $3 \cdot 10^{-7}$ - $15 \cdot 10^{-7} \text{ m}^3/\text{s}$, corresponding to primary channel inlet velocity from 0.2-1.0 m/s. Similar to that employed by Lee *et al.* [11], a constant heat flux of $6.5 \cdot 10^5 \text{ W/m}^2$ is applied at the base surface of DL-MCHS. Unless mentioned otherwise, this heat flux value is consistently employed in this numerical study. System coupling was used at the interface between solid and liquid domains interaction, and the top surface was assumed to be perfectly insulated. The boundary conditions imposed were summarized in tab. 2.

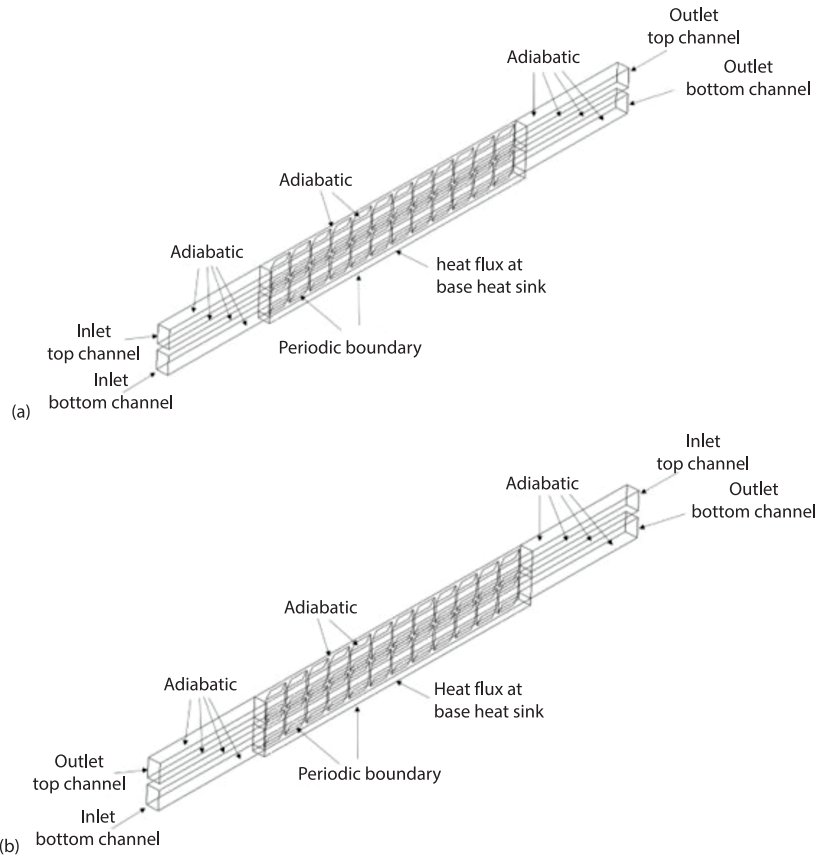


Figure 2. Geometry and boundary conditions of (a) a PF oblique finned DL-MCHS and (b) a CF oblique finned DL-MCHS

Table 2. Summary of boundary conditions imposed

	Hydrodynamic boundary condition	Thermal boundary condition
Inlet (top and bottom)	Constant velocity	Temperature 293 K
Outlet (top and bottom)	Pressure outlet	
Top surface	No-slip wall	Adiabatic (zero heat flux)
Solid and liquid interface	No-slip wall	System coupling
Base surface	No-slip wall	Constant heat flux $6.5 \cdot 10^5 \text{ W/m}^2$

Governing equations

To simulate the nanofluids in oblique finned DL-MCHS, single phase model is employed. The governing equations of the single phase model are given [20]:

– Continuity equation

$$\nabla(\rho_{\text{nf}} \vec{V}) = 0 \quad (1)$$

– Conservation of momentum

$$\nabla(\rho_{nf} \vec{V} \vec{V}) = -\nabla p + \nabla(\mu_{nf} \nabla \vec{V}) \quad (2)$$

– Energy equation

$$\nabla(\rho_{nf} \vec{V} c_{nf} T) = \nabla(k_{nf} \nabla T) \quad (3)$$

The density, pressure, and dynamic viscosity are denoted by ρ , p , and μ , respectively. Meanwhile, \vec{V} is the velocity field. The temperature, specific heat capacity and thermal conductivity are represented by T , c , and k , respectively. The subscript nf refers to nanofluids. The model is assumed to be incompressible and viscous dissipation is neglected. The integrated effects of momentum and energy exchange with base fluid was neglected.

For the solid substrate, the energy equation is given:

$$0 = \nabla(k_s \nabla T) \quad (4)$$

where k_s is the thermal conductivity of the solid substrate.

Thermophysical properties of fluid

In this study, the water properties are assumed to be temperature-dependent [21] where ρ_{bf} is density, k_{bf} is thermal conductivity, μ_{bf} represents fluid viscosity, and c_{bf} represents specific heat capacity of water. The properties of temperature-dependent of water are given [21]:

$$\rho_{bf} = 999.79 + 0.068(T - 273) - 0.0107(T - 273)^2 + 0.00082(T - 273)^{2.5} - 2.303 \cdot 10^{-5} (T - 273)^3 \quad (5)$$

$$k_{bf} = 0.56112 + 0.00193(T - 273) - 2.601 \cdot 10^{-6} (T - 273)^2 - 6.08 \cdot 10^{-8} (T - 273)^3 \quad (6)$$

$$\mu_{bf} = 0.00169 - 4.25 \cdot 10^{-5} (T - 273) + 4.92 \cdot 10^{-7} (T - 273)^2 - 2.09 \cdot 10^{-9} (T - 273)^3 \quad (7)$$

$$c_{bf} = 4217.4 - 5.61(T - 273) + 1.299(T - 273)^{1.52} - 0.11(T - 273)^2 + 4149.6 \cdot 10^{-6} (T - 273)^{2.5} \quad (8)$$

where T [K] represents temperature.

Meanwhile, constant thermophysical properties of Al_2O_3 are assumed [21] with density $\rho_p = 3.970 \cdot 10^3$ kg/m³, specific heat $c_p = 880$ J/kgK and thermal conductivity $k_p = 36$ W/mK:

– Density

The density of nanofluids, ρ_{nf} , is computed using mixture rule [22]:

$$\rho_{nf} = \rho_{bf}(1 - \phi) + \rho_p \phi \quad (9)$$

where ϕ is the volume fraction of nanoparticles, subscript nf, bf, and p are the nanofluid, base fluid, and nanoparticle.

– Specific heat

The effective specific heat of the nanofluid, c_{nf} , was calculated using the following equation [22], assuming thermal equilibrium between base fluid and nanoparticles:

$$c_{nf} = \frac{(1 - \phi)(\rho c)_{bf} + \phi(\rho c)_p}{\rho_{nf}} \quad (10)$$

– Thermal conductivity and viscosity

The thermal conductivity, k_{nf} , of Al_2O_3 - H_2O nanoparticles nanofluid was calculated based on equation proposed by Heyhat's experimental work [23] where it was fitted to the experimental results using a correlation coefficient of 0.95. In addition, Heyhat *et al.* [23] had also formulated the effective dynamic viscosity, μ_{nf} , equation of Al_2O_3 - H_2O nanofluids, as given in eq. (7):

$$k_{nf} = (1 + 8.733\phi)k_{bf} \quad (11)$$

$$\mu_{nf} = \mu_{bf} e^{\frac{5.989\phi}{0.278 - \phi}} \quad (12)$$

The governing equations of mass, momentum, and energy are solved using finite volume method via ANSYS FLUENT 18.1. Semi-implicit method for pressure-linked equations (SIMPLE) is used as the pressure-velocity coupling scheme. Second-order scheme is employed for pressure discretization while second-order upwind scheme is used for momentum and energy. Single-phase method for working liquid was employed using UDF to represent the nanofluids thermophysical properties. The convergence criterion with scaled residuals of 10^{-3} for continuity and momentum equations are used. Meanwhile, scaled residual of 10^{-6} is employed for energy equation. The thermal performance is assessed by the overall thermal resistance in the conjugate heat transfer model which is given:

$$R = \frac{T_{max} - T_{in}}{q'' A_b} \quad (13)$$

where T_{max} [K] is the maximum temperature of the heated surface, T_{in} [K] – the inlet temperature of the coolant, q'' – the heat flux applied at the base heat sink, and A_b – the surface area of the heat sink base.

On the other hand, the pumping power required in the DL-MCHS is calculated using eq. (14) to evaluate the pressure drop losses across the DL-MCHS. The pressure drop of coolant across MCHS (over the length of 25 mm) is denoted by Δp while \dot{V} is the volume flow rate of the coolant. Subscripts b and t represent bottom and top channels of double-layered MCHS, respectively:

$$P = \Delta p_b \dot{V}_b + \Delta p_t \dot{V}_t \quad (14)$$

Results and discussion

Validation of numerical simulation

The numerical model was first validated for counter flow conventional DL-MCHS. For conventional DL-MCHS, parallel-plate fins are employed. It should be noted that the geometric parameters for counter flow conventional DL-MCHS were adopted from the study of Wu *et al.* [24]. The 3-D numerical model was simulated for water (as the coolant fluid) with inlet velocity ranging between 1.0-3.5 m/s. Uniform heat flux, q'' , of $2 \cdot 10^6$ W/m² applied at the base silicon solid substrate materials. The simulated results attained are directly compared with the data reported by Wu *et al.* [24]. The comparison on overall thermal resistance and pumping power are illustrated in fig. 3. Both results are in good agreement with deviation less than 4%.

Grid independence test

A multi-zone with hexahedral mesh was adopted in this study. Four different mesh resolutions were employed with number of elements used are $1.35 \cdot 10^5$, $1.64 \cdot 10^5$, $1.84 \cdot 10^5$, and $2.1 \cdot 10^5$. For this grid independence test, the primary channel inlet velocity of 0.2 m/s is

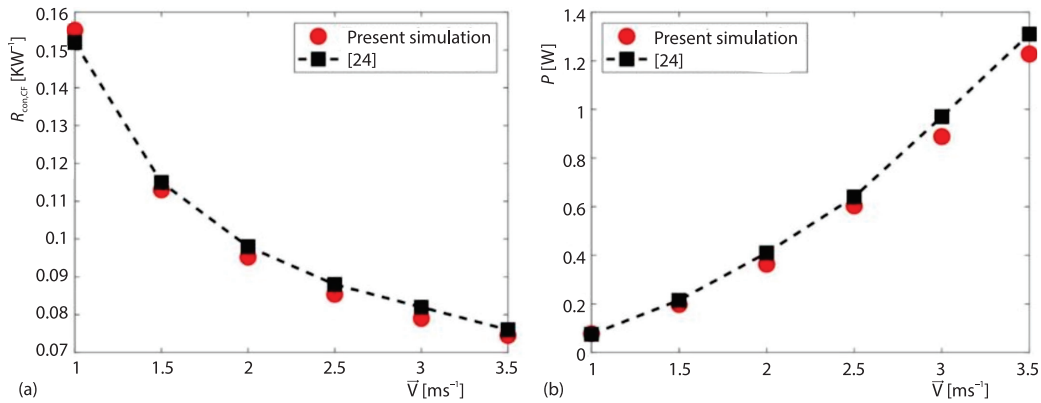


Figure 3. Comparison on (a) overall thermal resistance and (b) pumping power, with respect to different inlet velocities for counter flow conventional DL-MCHS with data of [24]

employed and water with temperature-dependent properties is used as the working liquid. The simulation results for the thermal resistance and pumping power requirement across the channel are shown in fig. 4. As indicated in this figure, numerical simulation with $1.84 \cdot 10^5$ elements yields sufficiently accurate results on both performances (overall thermal resistance and pumping power requirement). As compared to that of $2.1 \cdot 10^5$ elements, it would only yield deviation less than 0.4% for both performances. Therefore, numerical simulation with mesh resolution having approximately $1.84 \cdot 10^5$ elements is deemed to be suitable to be employed in this study and thus used hereafter.

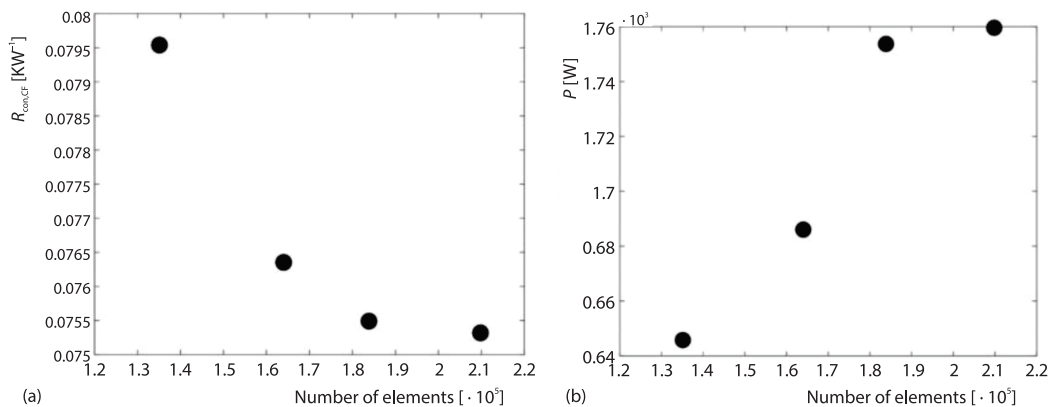


Figure 4. Grid independence test on (a) overall thermal resistance and (b) pumping power for cross-flow oblique finned DL-MCHS

Heat transfer performance with oblique finned DL-MCHS

Using pure water as the working liquid (in the absence of Al_2O_3 nanoparticles), the heat transfer performance of the oblique finned DL-MCHS is assessed. At a constant inlet velocity (*i.e.*, 0.2 m/s), the temperature distribution within the solid substrate for different heat sink designs and flow orientations, are illustrated in fig. 5. As can be deduced from this figure, hot region is located at the bottom surface, arising from the heat source imposed. For conventional DL-MCHS, parallel flow yields increasing temperature of solid substrate from inlet to

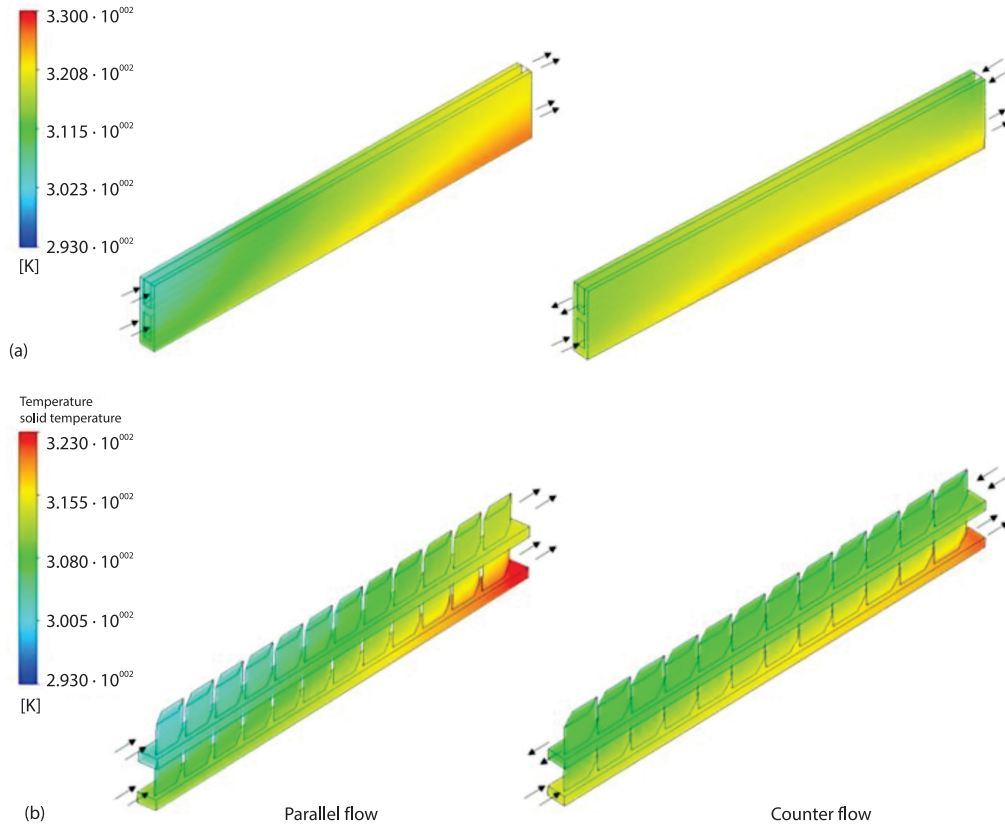


Figure 5. Temperature contour plot of solid substrate for (a) conventional DL-MCHS and (b) oblique finned DL-MCHS using water at 0.2 m/s inlet velocity

outlet while highest temperature for counter flow is located at the middle section in bottom surface. This is consistent with the observation made by Vafai and Zhu [2] and Wei *et al.* [3]. For oblique finned DL-MCHS, highest temperature is observed at the outlet of bottom surface, regardless of flow orientations (parallel and counter flows).

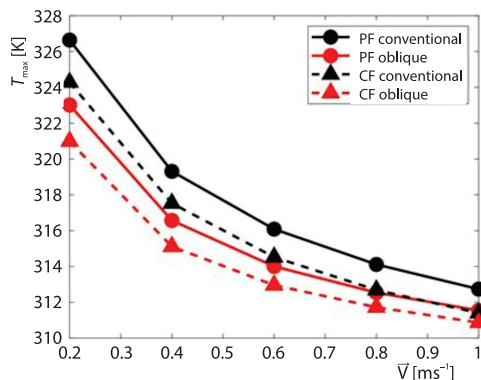


Figure 6. Maximum temperature at bottom surface of DL-MCHS with different inlet velocities

Comparing between conventional and oblique finned designs, the latter design consistently yields smaller maximum temperature, regardless of flow orientation and inlet velocity, as can be seen in fig. 6. This is mainly due to the fact that the temperature is more uniformly distributed across the oblique finned DL-MCHS than the conventional design due to better fluid mixing that is induced by the oblique finned channels as previously observed by Lee *et al.* [11]. Also, it is worth to note that cross-flow oblique finned DL-MCHS would consistently yield lower maximum temperature as compared

to its parallel flow counterpart. In addition, at a constant heat flux, the temperature distribution of the heat sink is significantly influenced by heat convection mechanism. When working liquid is forced at higher flow rate (*i.e.*, higher inlet velocity), the maximum temperature at the bottom surface significantly reduced. For example, at primary channel inlet velocity of 0.2 m/s, the maximum temperature is 320.98 K using cross-flow oblique finned DL-MCHS. The maximum temperature can be reduced to 310.87 K when fluid is forced at 1.0 m/s, using the same heat sink design.

Heat transfer enhancement with Al_2O_3 nanofluid

Apart from having water as the working liquid, this study also investigates the addition of Al_2O_3 nanoparticles. Based on the maximum temperature obtained from the numerical simulations, the overall thermal resistance is calculated via eq. (13). In this study, three different parameters of Al_2O_3 nanoparticles volume fraction (*i.e.*, 0%, 1%, and 4%) in water based nanofluids were considered. The resulted overall thermal resistance for both conventional and oblique finned DL-MCHS is plotted in fig. 7. For both heat sink configurations, the resulted overall thermal resistance is found to be significantly reduced in the presence of Al_2O_3 nanoparticles. The reduction in the overall thermal resistance is progressively dependent on the nanoparticles volume fraction. This is consistent, regardless of the flow orientations and heat sink designs investigated. The lowest overall thermal resistance of 0.0398 K/W is predicted using cross-flow oblique finned DL-MCHS with 4% volume fraction of Al_2O_3 nanoparticles. This is achieved at inlet velocity of 1 m/s.

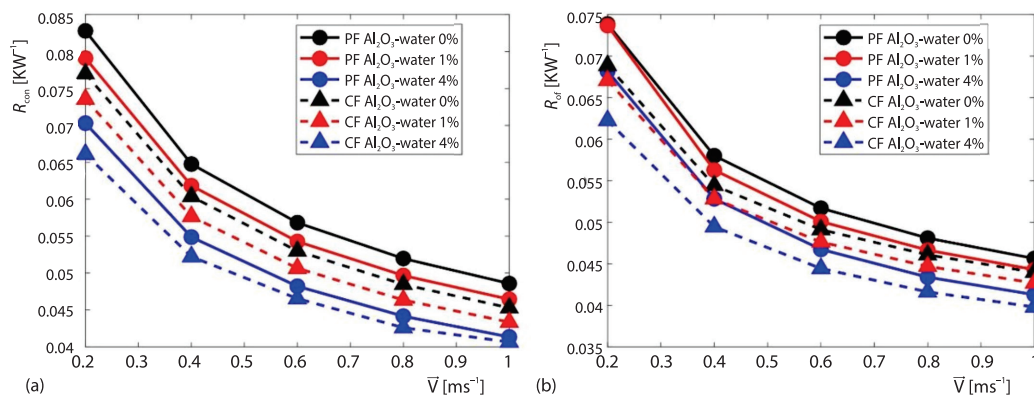


Figure 7. Dependency of overall thermal resistance with inlet velocity for (a) conventional DL-MCHS and (b) oblique finned DL-MCHS

To assess the heat transfer enhancement made by oblique finned DL-MCHS, the percentage of reduction in the overall thermal resistance is calculated via $\Delta R/R_{con,PF} \times 100\%$, as shown in fig. 8. The conventional DL-MCHS with parallel flow is taken as the baseline case. It is visible that cross-flow oblique finned DL-MCHS with 4% volume fraction of Al_2O_3 nanoparticles yields the best heat transfer enhancement, amongst all cases investigated. Using this heat sink configuration, the largest reduction in the overall thermal resistance can reach up to 25% with nanofluids flowing at 0.2 m/s. This is mainly owing to the superior thermal conductivity of the nanofluids. With 4% volume fraction of Al_2O_3 nanoparticles, the effective thermal conductivity is almost 35% larger than that of pure water, thereby enhancing the convective heat transfer mechanism and then reducing the overall thermal resistance of the conjugate heat transfer system. However, the $\Delta R/R_{con,PF}$ is found to be dependent on the flow rate with smaller thermal enhancement is pre-

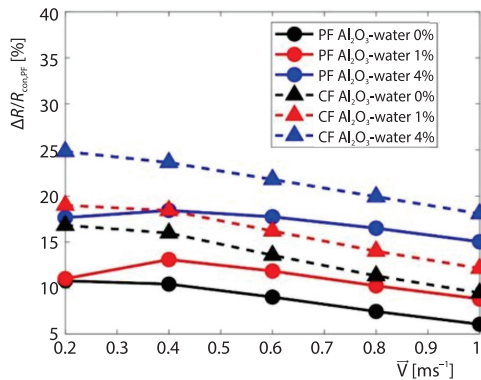


Figure 8. Percentage of reduction in the overall thermal resistance for oblique finned DL-MCHS at different inlet velocities

dicted for higher fluid velocity, even though the same heat sink design is used. As can be observed from fig. 8, $\Delta R/R_{\text{con,PF}}$ is almost linearly reduced with respect to fluid velocity, in particularly for cross-flow configuration. With higher flow velocity, the fluid convection is more substantial, thus resulting in more flow rate passing through the primary channel. In other words, forced convection heat transfer through the secondary channel is thus weakened, thereby reducing the heat transfer enhancement of oblique fin at higher inlet flow, causing $\Delta R/R_{\text{con,PF}}$ to reduce. In addition, it is worth to note that double-layered heat sink design with cross-flow configuration would yield better thermal enhancement as compared to its parallel flow counterpart.

Pumping power

Apart from assessing the heat transfer performance, the pumping power required for the oblique finned DL-MCHS is also evaluated. Numerical simulations predicted that increasing pumping power is required when flow velocity across the channel increases. As shown in fig. 9, the increasing trend on pumping power with respect to inlet velocity can be observed in all cases investigated. It is interesting to note that heat sink designs with parallel flow and counter flow would yield almost similar pumping power requirement. This would imply that for double-layered heat sink, the thermal performance can be simply improved by using counter flow configuration (instead of having parallel flow configuration), without having additional pressure drop losses. Using nanofluids, as expected, the addition of nanoparticles into water would increase the fluid viscosity, thereby causing higher frictional losses between fluid-flow and the wall boundary. For oblique finned DL-MCHS, when 4% volume concentration nanofluids is used, the pumping power is approximately twice higher than that of water.

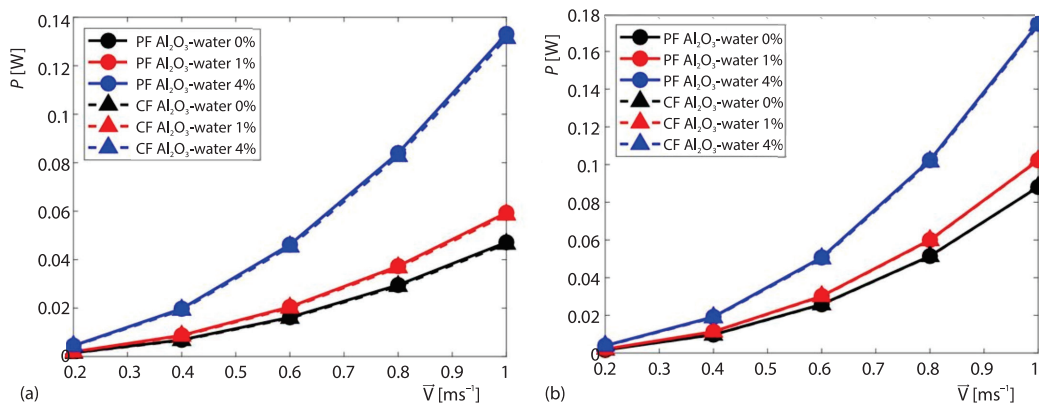


Figure 9. Dependence of pumping power requirement with inlet velocity in (a) conventional DL-MCHS and (b) oblique finned DL-MCHS

Conclusion

In the present study, conjugate heat transfer simulation of nanofluid in laminar flow regime with volume flow rate of $3 \cdot 10^{-7}$ to $15 \cdot 10^{-7}$ m³/s was investigated at 0%, 1%, and 4% volume concentration of Al₂O₃ nanoparticles in oblique finned DL-MCHS design. The thermal resistance of the heat sink system decreases as the volume concentration of nanoparticles increases, applicable for both parallel flow and counter flow configuration. Lowest thermal resistance is observed in oblique finned DL-MCHS in counter flow configuration with 4% volume concentration of nanofluids, with $R = 0.0398$ K/W. Using this configuration, largest reduction in the overall thermal resistance can reach up to 25% with nanofluids flowing at 0.2 m/s. Comparatively, counter flow configuration offers lower thermal resistance, for all nanofluids volume concentrations investigated. The lower thermal resistance observed in oblique finned DL-MCHS is mainly owing to the better convective heat transfer mechanism. This leads to a more uniform temperature distribution across the oblique finned DL-MCHS than that of the conventional design. Despite the promising heat transfer enhancement of the oblique finned DL-MCHS, additional pumping power is expected.

Acknowledgment

The authors acknowledge the Ministry of Education (MOE) of Malaysia under Fundamental Research Grant Scheme (FRGS Grant No. FRGS/1/2019/TK03/USM/03/3).

Nomenclature

A – surface area, [m²]
 c – specific heat, [Jkg⁻¹K⁻¹]
 k – thermal conductivity, [Wm⁻¹K⁻¹]
 P – pumping power, [W]
 p – pressure, [Pa]
 q'' – heat flux, [Wm⁻²]
 R – thermal resistance, [KW⁻¹]
 T – temperature, [K]
 \vec{V} – velocity, [ms⁻¹]
 \dot{V} – volume flow rate, [m³s⁻¹]

Greek symbol

ρ – density, [kgm⁻³]
 μ – dynamic viscosity, [kgm⁻¹s⁻¹]
 ϕ – volume fraction of nanoparticles, [-]

Subscripts

b – bottom
 bf – base fluid
 CF – counter flow
 con – conventional
 in – inlet
 max – Maximum value
 nf – Nanofluid
 PF – parallel flow
 p – particle
 s – solid
 t – top

References

- [1] Tuckerman, D. B., Pease, R. F. W., High-Performance Heat Sinking for VLSI, *IEEE Electron Device Letters*, 2 (1981), 5, pp. 126-129
- [2] Vafai, K., Zhu, L., Analysis of Two-Layered Micro-Channel Heat Sink Concept in Electronic Cooling, *International Journal of Heat and Mass Transfer*, 42 (1999), 12, pp. 2287-2297
- [3] Wei, X., *et al.*, Experimental and Numerical Study of a Stacked Micro-channel Heat Sink for Liquid Cooling of Microelectronic Devices, *Journal of Heat Transfer*, 129 (2007), 10, pp. 1432-1444
- [4] Ansari, D., Kim, K. Y., Performance Analysis of Double-Layer Micro-Channel Heat Sinks under Non-Uniform Heating Conditions with Random Hotspots, *Micromachines*, 8 (2017), 2, 54
- [5] Deng, D., *et al.*, Numerical Study of Double-Layered Micro-channel Heat Sinks with Different Cross-Sectional Shapes, *Entropy*, 21 (2019), 1, 16
- [6] Hung, T.-C., *et al.*, Analysis of Heat Transfer Characteristics of Double-Layered Micro-Channel Heat Sink, *International Journal of Heat and Mass Transfer*, 55 (2012), 11, pp. 3090-3099

- [7] Xie, G., et al., Numerical Predictions of the Flow and Thermal Performance of Water-Cooled Single-Layer and Double-Layer Wavy Micro-channel Heat Sinks, *Numerical Heat Transfer – Part A: Applications*, 63 (2013), 3, pp. 201-225
- [8] Ansari, D., Kim, K.-Y., Double-Layer Micro-Channel Heat Sinks with Transverse-Flow Configurations, *Journal of Electronic Packaging*, 138 (2016), 3, 031005
- [9] Toh, K. C., et al., Numerical Computation of Fluid-flow and Heat Transfer in Micro-Channels, *International Journal of Heat and Mass Transfer*, 45 (2002), 26, pp. 5133-5141
- [10] Knight, R.W., et al., Heat Sink Optimization with Application Micro-channels, *IEEE Transactions on Components, Hybrids, and Manufacturing Technology*, 15 (1992), 5, pp. 832-842
- [11] Lee, Y. J., et al., Enhanced Thermal Transport in Micro-channel Using Oblique Fins, *Journal of Heat Transfer*, 134 (2012), 10, 101901
- [12] Lee, Y. J., et al., Numerical Study of Fluid-Flow and Heat Transfer in the Enhanced Micro-Channel with Oblique Fins, *Journal of Heat Transfer*, 135 (2013), 4, 041901
- [13] Pak, B. C., Cho, Y. I., Hydrodynamic and Heat Transfer Study of Dispersed Fluids with Submicron Metallic Oxide Particles, *Experimental Heat Transfer*, 11 (1998), 2, pp. 151-170
- [14] Vajjha, R. S., Das, D. K., A Review and Analysis on Influence of Temperature and Concentration of Nanofluids on Thermophysical Properties, Heat Transfer and Pumping Power, *International Journal of Heat and Mass Transfer*, 55 (2012), 15, pp. 4063-4078
- [15] Chein, R., Chuang, J., Experimental Micro-Channel Heat Sink Performance Studies Using Nanofluids, *International Journal of Thermal Sciences*, 46 (2007), 1, pp. 57-66
- [16] Iqbal, S. M., et al., A Comparative Investigation of $\text{Al}_2\text{O}_3/\text{H}_2\text{O}$, $\text{SiO}_2/\text{H}_2\text{O}$ and $\text{ZrO}_2/\text{H}_2\text{O}$ Nanofluid for Heat Transfer Applications, *Digest Journal of Nanomaterials and Biostructures*, 12 (2017), 2, pp. 255-263
- [17] Ting, H.-H., Hou, S.-S., Numerical Study of Laminar Flow and Convective Heat Transfer Utilizing Nanofluids in Equilateral Triangular Ducts with Constant Heat Flux, *Materials*, 9 (2016), 7, 576
- [18] Ting, H.-H., Hou, S.-S., Numerical Study of Laminar Flow Forced Convection of Water- Al_2O_3 Nanofluids under Constant Wall Temperature Condition, *Mathematical Problems in Engineering*, 2015 (2015), ID180841
- [19] Tiwary, B., et al., Heat Transfer Enhancement in Oblique Finned Channel, *Lecture Notes in Mechanical Engineering*, (2019), Apr., pp. 157-167
- [20] Bianco, V., et al., Numerical Investigation of Nanofluids Forced Convection in Circular Tubes, *Applied Thermal Engineering*, 29 (2009), 17, pp. 3632-3642
- [21] Purohit, N., et al., Assessment of Nanofluids for Laminar Convective Heat Transfer: A Numerical Study, *Engineering Science and Technology, an International Journal*, 19 (2016), 1, pp. 574-586
- [22] Khanafer, K., Vafai, K., A Critical Synthesis of Thermophysical Characteristics of Nanofluids, *International Journal of Heat and Mass Transfer*, 54 (2011), 19, pp. 4410-4428
- [23] Heyhat, M. M., et al., Experimental Investigation of Laminar Convective Heat Transfer and Pressure Drop of Water-Based Al_2O_3 Nanofluids in Fully Developed Flow Regime, *Experimental Thermal and Fluid Science*, 44 (2013), Jan., pp. 483-489
- [24] Wu, J. M., et al., Parametric Study on the Performance of Double-Layered Micro-channels Heat Sink, *Energy Conversion and Management*, 80 (2014), Apr., pp. 550-560